ACS Sustainable Chemistry & Engineering

Research Article

pubs.acs.org/journal/ascecg

ZnO Superstructures as an Antifungal for Effective Control of *Malassezia furfur*, Dermatologically Prevalent Yeast: Prepared by Aloe Vera Assisted Combustion Method

D. Kavyashree,[†] C. J. Shilpa,[‡] H. Nagabhushana,*[,‡] B. Daruka Prasad,[§] G. L. Sreelatha,[∥] S. C. Sharma,[⊥] S. Ashoka,[#] R. Anandakumari,[⊗] and H. B. Premkumar[▽]

[†]Department of Physics, Channabasaveshwara Institute of Technology, Visveswaraya Technological University, Gubbi 572216, India

[‡]Prof. C.N.R Rao Centre for Advanced Materials, Tumkur University, Tumkur 572103, India

[§]Department of Physics, B.M.S. Institute of Technology, Visveswaraya Technological University, Bangalore 560064, India

[∥]Department of Microbiology & Biotechnology, Bangalore University, Jnana Bharathi Campus, Bangalore 560056, India

[⊥]Dayananda Sagar University, Shavige Malleshwara Hills, Kumaraswamy Layout, Bangalore 560078, India

[#]Department of Chemistry, Post Graduate Center, Vijaya College, R.V. Road, Bangalore 560004, India

[⊗]Department of Physics, Sree Siddaganga College for Women, Tumkur 572103, India

[▽]Department of Physics, Acharya Institute of Technology, Bangalore 560090, India

ABSTRACT: In this paper, a robust and simple biogenic route has been developed to synthesize self-assembled ZnO superstructures in short intervals of time using naturally available aloe vera plant gel and zinc nitrate as starting materials. The stabilization of zinc ions with polysaccharides wrapped chains along with the support of proteins, lipids and physterols of aloe vera gel followed by combustion derives the ZnO superstructures. The obtained ZnO superstructures show a hexagonal crystal phase and exhibit a semiconducting behavior with the energy band gap varies from 2.92 to 3.08 eV. The aloe vera gel derived ZnO superstructures exhibit unique and strong orange-red emission centered at 600 nm. The better structural, morphological and photoluminescence results are obtained for ZnO prepared with 16.6% W/V of zinc nitrate with aloe vera content compared to other concentrations of aloe vera. The prepared compounds are tested for antimalassezial activity against *Malassezia furfur*, dermatologically prevalent yeast, and were found to have minimum inhibitory concentration (MIC) values ranging from 8 to 125 μg/mL. Fluorescence microscopic analysis revealed that yeast cells treated with ZnO superstructures have the chromatin as orange instead of green, showcasing the cell aggregation suggests that ZnO superstructures have an immense potential as an antifungal agent. Hence, the explored method of preparation shows high efficient ZnO superstructures derived from the aloe vera plant gel have potential applications in the medical, biomedical and cosmetic industries.

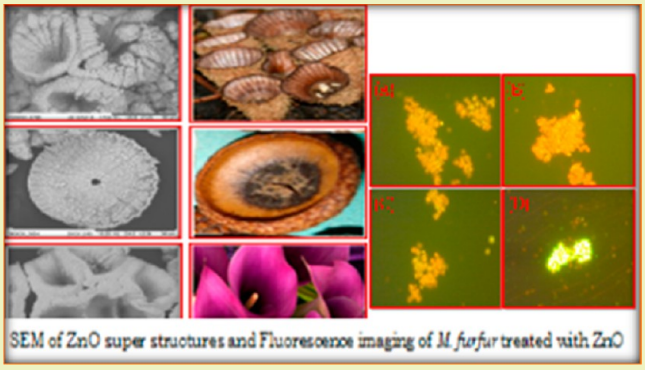

SEM of ZnO super structures and Fluorescence imaging of *M. furfur* treated with ZnO

KEYWORDS: *Zinc oxide superstructures, Green synthesis, Photoluminescence, Antidandruff, Antimalassezial activity*

INTRODUCTION

Dandruff is a common embarrassing scalp disorder affecting a large portion of the population. It is caused due to excessive flaking of dead skin cells from the scalp. Recent finding confirmed that *Malassezia furfur* (*M. furfur*), lipophilic, saprophytic and basidiomycetous yeast, belonging to resident flora of human skin,[1] have been responsible for the pathogenesis of several chronic diseases such as pityriasisversicolor,[2] folliculitis[3] and seborrhoeic dermatitis,[4] and some forms of atopic dermatitis,[5] psoriasis[6] and confluent and reticulate papillomatosis.[7] It has been isolated from sebum-rich areas of the body such as the upper trunk, head and face.

M. furfur has special requirements for exogenous lipids due to its inability to synthesize long-chain fatty acids.[8] The topical and systemic treatments available today typically do not eradicate but only help in reinstating the yeast's population. The available active ingredients included in treatment options are zinc pyrithione, salicyclic acid, corticosteroids, imidazole derivatives, glycolic acid, steroids, selenium suplhide and sulfur coal tar derivatives. These drugs are toxic and expensive and require

Received: December 17, 2014
Revised: April 29, 2015
Published: May 4, 2015

DOI: 10.1021/sc500784p
ACS Sustainable Chem. Eng. 2015, 3, 1066−1080

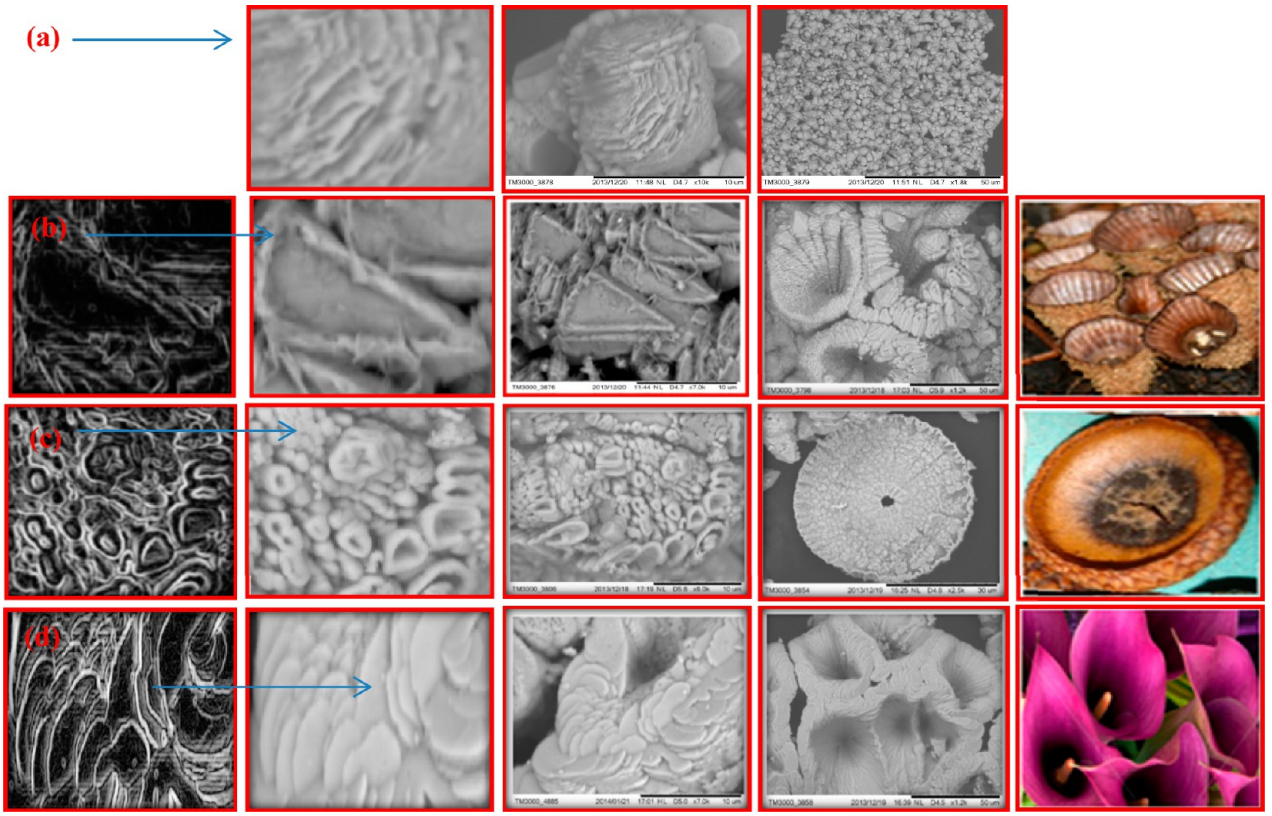

Figure 1. SEM images of the ZnO-SS synthesized using aloe vera gel of different concentrations: (a) without aloe vera gel, (b) 50% W/V zinc nitrate with aloe vera gel, (c) 25% W/V zinc nitrate with aloe vera gel and (d) 16.6% W/V zinc nitrate with aloe vera gel.

prolonged treatment.[9] Therefore, it is imperative to develop alternative antifungal agents with versatile features such as an effective combination of antimicrobial potency, wide availability, less toxicity and good compatibility.

In this view, nanostructured metal oxides have gained intensive interest, due to their electrostatic attraction between negatively charged microbial cells and positively charged nanoparticles for the activity of nanoparticles as antifungal agents.[10,11] These materials have the potential to revolutionize medicine because of their ability to interact at molecular and cellular levels of organs and tissues of a human body.[12] Their unique size dependent properties make these materials superior and indispensable in many more areas of research like solar cells,[13] gas sensors,[14] photosensors,[15,16] piezoelectric devices,[17] waste water treatment[18] and so on. The nanostructures were already tested for their antimicrobial properties as antibacterial, antifungal and antiyeast.[19−22] Thus, innovative and scalable synthesis routes need to be developed to control the production and morphology of the various metal oxides on nano- and microscales.

Several synthesis approaches have been successfully explored for the controlled synthesis of a variety of ZnO superstructures (ZnO-SS) viz. spray-pyrolysis, precipitation, hydrothermal, chemical vapor deposition, sol−gel, thermal evaporation, solution combustion, etc.[23−30] Chemical procedures involved in these synthesis methods produce the main products and also release the hazardous waste products to the environment. Thus, there is a need for "green chemistry", which includes clean, nontoxic and environmentally benign routes. Additionally, the large-scale synthesis of pure ZnO-SS with unique properties at relatively low temperatures still remains a challenge.

As a result, developing a simple and fast synthesis route that can control the shape and size of ZnO-SS with high yield under ambient conditions has received significant attention. The use of naturally available plant based materials such as leaf, root, latex, seed and stem appear to be the best for large scale synthesis.[31−35] The aloe vera plant gel, which has many health benefits, has been attributed to the polysaccharides contained in the gel of the leaves. These biological entities help in wound healing, antifungal activity, hypoglycaemic, anticancer and immunomodulatory properties. This plant gel has been previously employed for the preparation of size and shape controlled metallic superstructures. However, the potential use of an aloe vera plant gel as a biotemplate for the synthesis of different ZnO-SS is not yet explored in detail.

Therefore, in this communication, we have employed modified solution combustion method for the production of self-assembled ZnO-SS using low cost and naturally available aloe vera plant gel. Aloe vera plant gel acts as a fuel, surfactant and as a sacrificial biotemplate. The overall synthesis time required for the preparation of self-assembled ZnO-SS is less than 20 min. The typical green synthesis involves the simple heat treatment of thoroughly mixed aqueous solution of the naturally available aloe vera plant and zinc nitrate at 300 °C. The prepared samples were further tested for the management of superficial infections caused by *M. furfur* yeast.

EXPERIMENTAL SECTION

All the chemicals used for the synthesis of ZnO-SS are of analytical grade and used without further purification. Zinc nitrate hexahydrate ($Zn(NO_3)_2{\cdot}6H_2O$; 99% pure) was procured from Sigma-Aldrich. Aloe vera plant gel was collected according to a previous literature reported by Patel et al.[35] The 20% V/V of pure aloe vera gel is mixed thoroughly with double distilled water and prepared the mother solution using a magnetic stirrer. The resulting aloe vera gel solution of different volumes

DOI: 10.1021/sc500784p
ACS Sustainable Chem. Eng. 2015, 3, 1066−1080

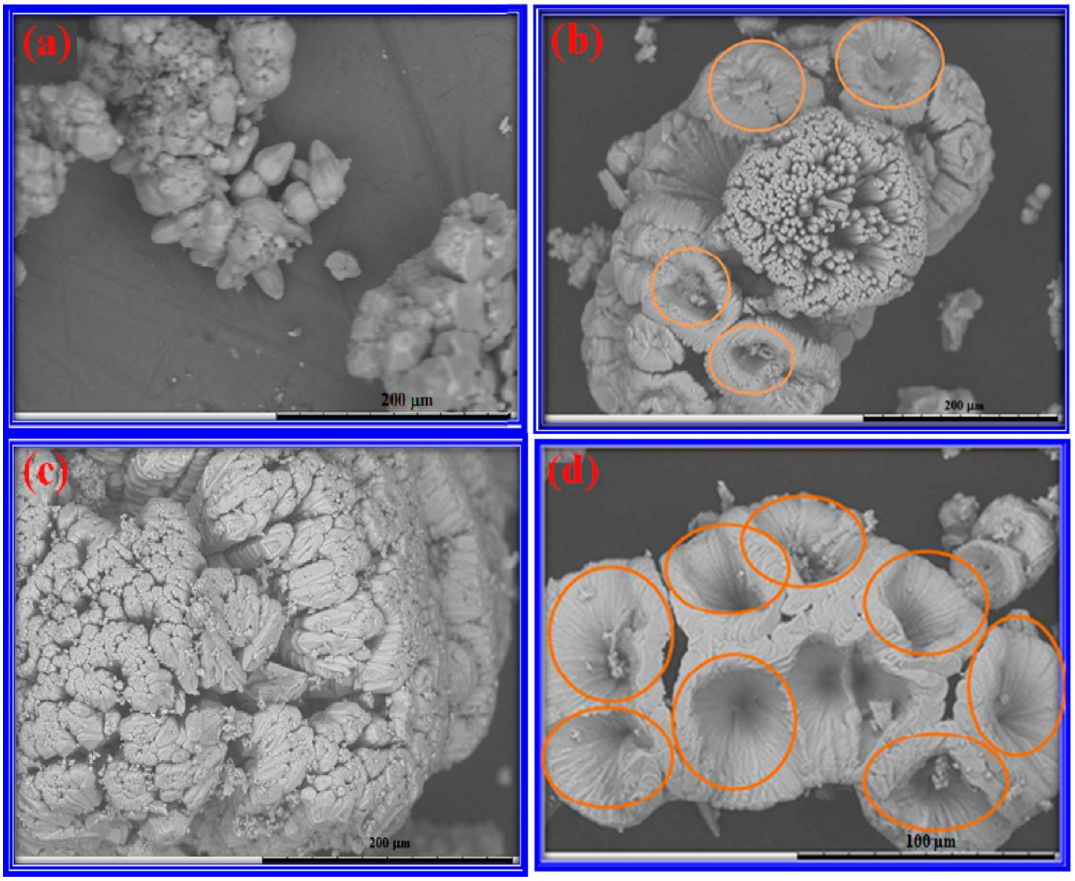

Figure 2. Large area SEM images of ZnO-SS obtained using various concentration of aloe vera gel: (a) without aloe vera gel, (b) 50% W/V zinc nitrate with aloe vera gel, (c) 25% W/V zinc nitrate with aloe vera gel and (d) 16.6% W/V zinc nitrate with aloe vera gel.

was used along with zinc nitrate hexahydrate for synthesis of ZnO-SS. In a typical synthesis, four numbers of concentrations are selected, one without the use of aloe vera to prepare ZnO where oxyalyldihyrazide is used as a fuel. The other three samples were prepared with concentrations of 50% W/V, 25% W/V and 16.6% W/V of zinc nitrate hexahydrate along with the above-mentioned mother solution containing aloe vera gel. The resulting solutions were stirred constantly by using a magnetic stirrer for ∼10 min. Then the obtained solutions were kept in a preheated muffle furnace maintained at 300 ± 10 °C. Within a few minutes, the solution caught fire and underwent smoldering type of burning and resulted in a foamy and bulged white powder. The powders were collected, characterized and tested for antifungal activity.

Microorganism, Media and Chemicals. Pure culture *M. furfur* (strain no. 1374) was obtained from Microbial Culture Collection Centre and Genebank (MTCC). The culture was maintained in modified Emmon's agar medium and Saborauds dextrose agar (SDA) supplemented with milk. Leeming–Notman agar (LNA) medium was used for carrying out antimicrobial studies. The plates were incubated at 32 ± 2 °C for 4 days.[36]

***In Vitro* Antimalassezial Susceptibility Assay.** Inoculum preparation was done by a direct colony suspension method recommended by National Committee for Clinical and Laboratory Standards (NCCLS). The disc diffusion assay was used to screen the antifungal activity of all the extracts. Inoculum suspension previously adjusted to 0.5 McFarland standard was swabbed evenly over the sterile LNA agar medium plates set for the disc diffusion assay. This procedure yielded a yeast stock suspension of 3×10^6 cells per mL and produced semiconfluent growth with *M. furfur*. Sterile 6 mm diameter discs were placed equidistantly round the margin of petridish. 10 μL of test samples (1 and 0.5 mg mL^{-1}) was dispensed on the discs. Ketoconazole was used as a positive reference standard. A negative control was prepared using the same solvent (ethanol) used to dissolve the test sample. The inoculated plates were incubated at 32 ± 2 °C for 48 h. Each test was performed in triplicate. The antifungal activity was evaluated by measuring the inhibition-zone diameter observed after 48 h of incubation.

Evaluation of Minimum Inhibitory Concentration (MIC) by Microbroth Dilution Assay. MICs were determined in 96-well microtitre well plates recommended by the National Committee for Clinical Laboratory Standards (NCCLS). The ZnO-SS/ZnO nanoparticles (without aloe vera) were diluted by 2-fold serial dilution ranging from 1 to 0.004 mg mL^{-1}. 100 μL of ZnO-SS solution was transferred into each well. 100 μL of standardized inoculum suspension (3×10^6 cells/mL) of yeast cells was added to the wells. The plates were then incubated at 32 ± 2 °C for 48 h. After 48 h of incubation, 15 μL of Iodonitrotetrazolium (INT) chloride was added in each well and further incubated for 4 h to obtain color change from colorless to purple. MICs were determined as the lowest concentration of the drug that prevented the color change. The standard reference used in these studies was ketoconazole at the concentration of 0.156 $mgml^{-1}$. A well was reserved in each plate as growth control and blank. The experiment was performed in triplicate under meticulous aseptic conditions.[37] The MFC was determined by inoculating the contents from the 96-well plates onto LNZ agar plates by streak method and the results were observed after 48 h incubation at 32 ± 2 °C. The lowest concentration of the NP that was able to kill the microorganisms was considered as the Minimum Yeast-cidal concentration (MYC).[37]

Fluorescence Microscopy Analysis. 100 μL of the inoculums suspension was incubated with 50 μL of minimal dosage of ZnO-SS, which favored inhibition of yeast cells. The cells were centrifuged at 6000 rpm for 10 min and washed twice with 1× phosphate buffered saline (PBS) and stained with Ethidium bromide and Acridine orange (EB/AO). An EB/AO stock solution (100 μg/mL) was prepared in Milli-Q water and stored in the dark at −20 °C.

DOI: 10.1021/sc500784p
ACS Sustainable Chem. Eng. 2015, 3, 1066–1080

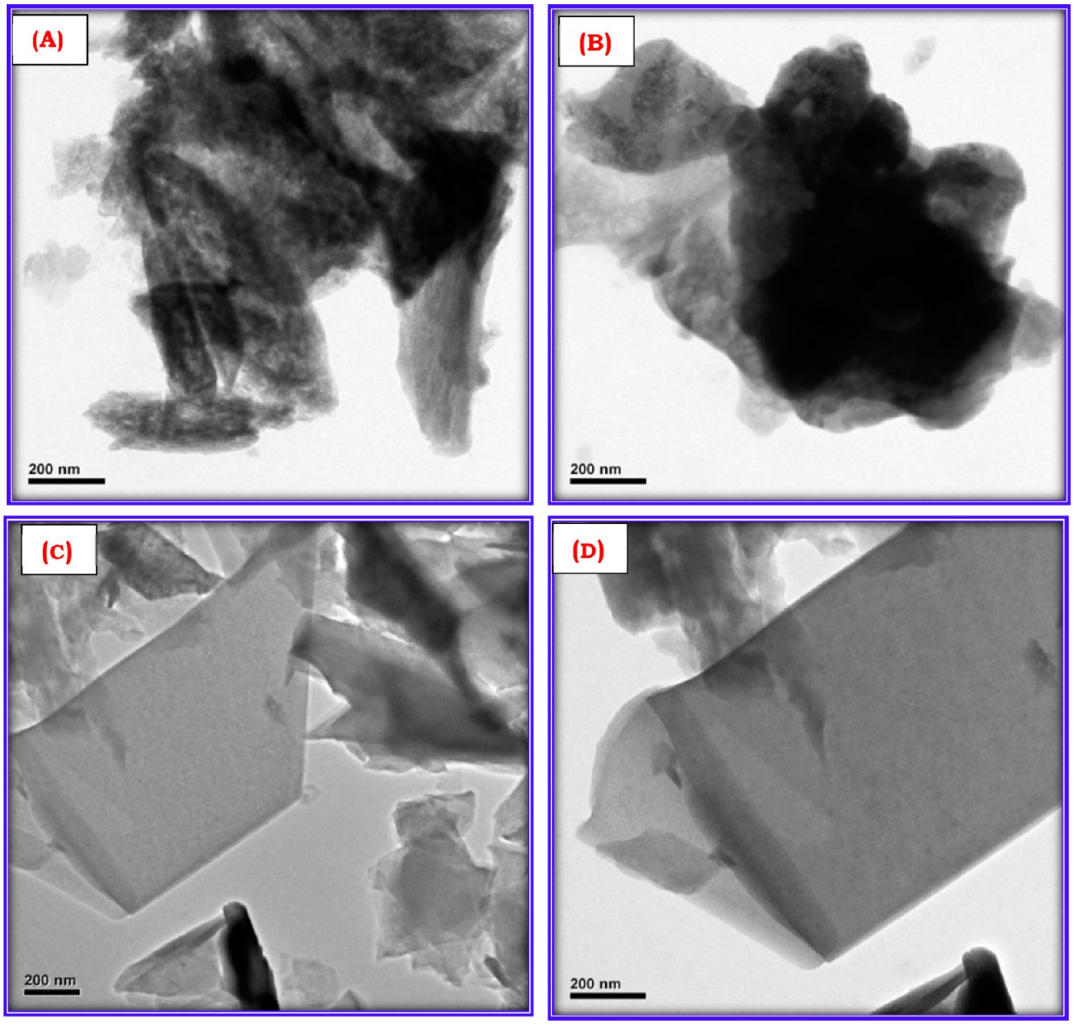

Figure 3. TEM images of ZnO prepared (A) without aloe vera gel, (B) 50% W/V, (C) 25% W/V and (D) 16.6% W/V zinc nitrate with aloe vera gel.

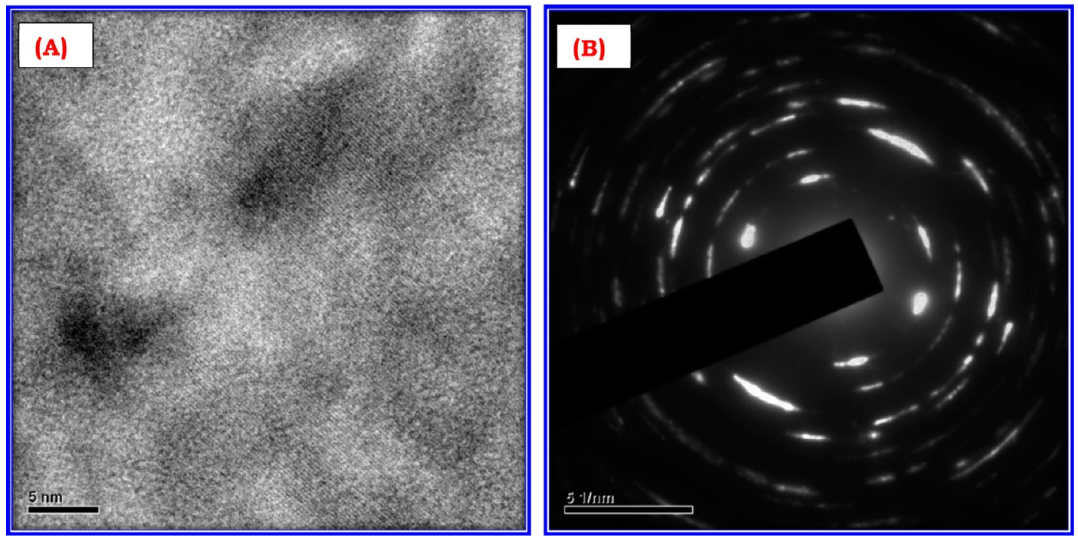

Figure 4. (A) HRTEM and (B) SAED pattern of ZnO prepared with 16.6% W/V zinc nitrate with aloe vera gel.

CHARACTERIZATION

The surface morphology of ZnO superstructures is characterized by scanning electron microscopy (SEM, Hitachi-3000). Transmission electron microscopy (TEM), high resolution transmission electron microscopy (HRTEM) and selected-area electron diffraction (SAED) pattern analyses were done using a JEOL 2100 HRTEM instrument. The crystal structure and composition of ZnO superstructures were determined by a

DOI: 10.1021/sc500784p
ACS Sustainable Chem. Eng. 2015, 3, 1066−1080

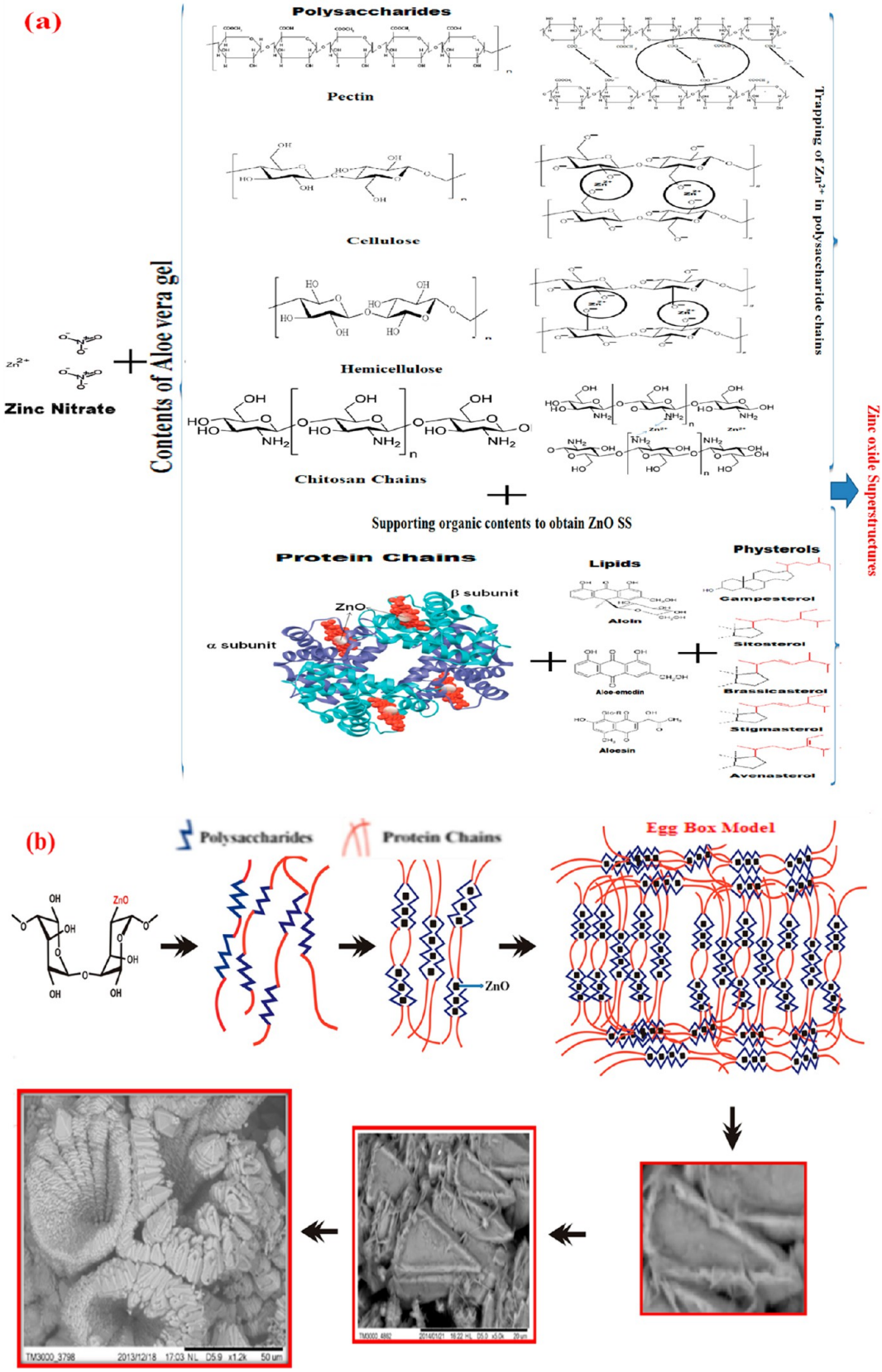

Figure 5. (A) Pictorial representation of contents of aloe vera gel and ZnO formation due to the trapping of Zn^{2+} with polysaccharide chains (B) pictorial representation of ZnO-SS formation according to the egg box model in the environment of aloe vera extract.

Shimadzu powder X-ray diffractometion (PXRD) instrument using Cu Kα radiation in the 2θ range of 20−80°. The X-ray photoelectron spectroscopy (XPS) of ZnO was examined using an ultrahigh vacuum setup equipped with a high resolution Gamma data-Scienta SES 2002 analyzer. The Fourier transform infrared (FTIR) spectrum was recorded in absorption mode with

DOI: 10.1021/sc500784p
ACS Sustainable Chem. Eng. 2015, 3, 1066−1080

Perkin Elmer spectrometer (Spectrum 1000) along with KBr pellets. The presence of organic and inorganic traces and their type of bonding are analyzed using FTIR. The UV−vis spectrum of the sample was recorded by dispersing the powder in liquid paraffin with the Specord S600-212C205 spectrometer. The optical properties were investigated with a Horiba Fluorolog spectrofluorimeter recorded at room temperature using a xenon lamp as the excitation source. The excitation wavelength of 325 nm was used.

Each ZnO-SS sample was mixed with a stock solution of fluorescent dye just prior to microscopy analysis, and the samples were incubated in the dark for 30 min. Morphology of exposed cells was determined under fluorescent microscopy analysis after labeling with EB/AO. 10 μL of cell suspension was placed onto a slide, covered with a glass coverslip and examined using a Carl Zeiss fluorescence microscope (excitation filter BP 490; barrier filter O 515), at 40× magnification.[38−40]

RESULTS AND DISCUSSION

SEM and TEM together provide detailed characterization to confirm the nanosize and to analyze the surface morphology/

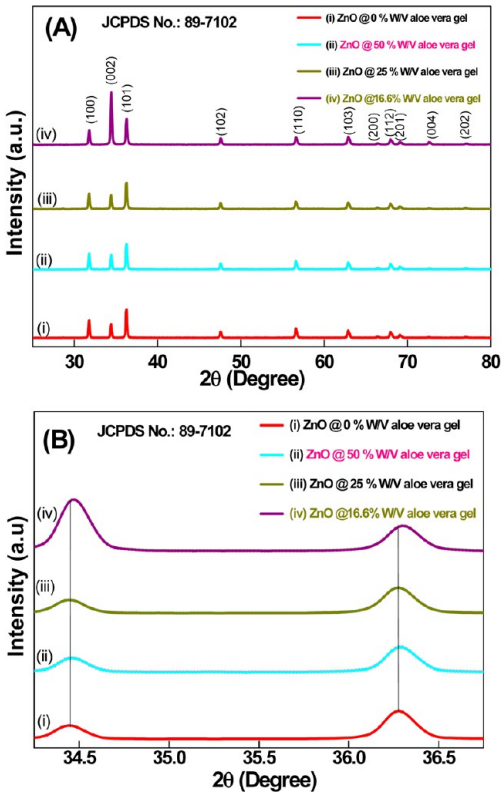

Figure 6. PXRD pattern of ZnO products with various concentrations of aloe vera gel content (A) the 2θ range from 20−80° and (B) the 2θ specific range of 34−37°.

particles size of the prepared ZnO compounds. The size and shape of the superstructures obtained represents the selected high and low magnified SEM images of the ZnO-SS with and without aloe vera gel (Figure 1, high magnification; Figure 2, low magnification). Simple decomposition of zinc nitrate in water has been carried out to compare the effect of aloe vera on ZnO nano/micro structure formation. The SEM image of ZnO prepared without aloe vera gel consists of strongly agglomerated flakes type structure (Figure 1a). Figure 1b−d shows the SEM images for ZnO prepared with varying concentrations of aqueous Zn $(NO_3)_3$ and aloe vera gel of 50% W/V, 25% W/V and 16.6% W/V respectively. The pictures observed in horizontal line of Figure 1 shows the digitized form of the selected portion of the image, selected portion of the image for digitization, image shown with 10 μm scale, image shown with 50/30 μm scale and the equivalent naturally existing picture.

The images clearly indicate that the micrographs are composed of several micro/nanoentities namely bowl and platelets. Figure 1b shows the SEM images of the ZnO prepared using 50% W/V zinc nitrate with aloe vera gel; the presence of well-ordered microstructures consists of pyramids organized one above the other resembles the group of layered nests. The other SEM images of the ZnO prepared using different concentrations of aloe vera gel consists of acoron caps and group of lily flowers respectively for 25% W/V and 16.6% W/V concentrations of zinc nitrate with aloe vera gel. The SEM image of the ZnO prepared using 16.6% W/V concentrated reaction mixture consists of clusters of symmetrically arranged small plates with superstructure resemblance to lily flowers (Figure 1d). This confirms that the aloe vera gel acts as a sacrificial biotemplate in the formation of ZnO-SS during combustion. To support for the formation of ZnO-SS, a number of similar types of superstructures in the larger area are shown in Figure 2 a−d. Figure 3A−D shows the TEM images of the four samples, the ZnO without aloe vera shows the loosely bounded particles of irregular shape, whereas the TEM images with different concentrations of aloe vera shows the increased bounding and flakes type ordered particles. Further, the nanosize of the particles is supported with HRTEM and indexed SAED pattern for the sample with highest aloe vera concentration (Figure 4A,B) shows well patterned *d*-spacing of 0.25 nm.

Aloe vera gel consists of several multifunctional organic compounds, which include water/moisture, soluble polysaccharides, monosaccharides, proteins, lipids, phytosterols, amino acids, glycoproteins, enzymes, vitamins such as ascorbic acid, complex B: thiamin, riboflavin, niacin, folic acid carotenoids and tocopherols.[41] Further, it also contains minerals and trace elements with some kind of gum materials. The active ingredient in aloe vera extraction is the polysaccharides. This shows stability in harsh environments associated with high temperature and pH. It shows affinity towards water and incorporates strongly in biological structure. When zinc nitrate mixed with aloe vera plant gel, the Zn^{2+} ions will distribute uniformly, thereby forming a three-dimensional polymeric network structure. The resulting polymeric networks undergo slow decomposition when subjected to heat treatment. Similar work has been reported by Maliyekkal et al.,[42] where cellulose is used as a template during the decomposition of magnesium nitrate in the mixture of urea and glycine to prevent the agglomeration and escape of combustion products from the reaction vessel. In addition, the formation of polymer network controls the combustion rate, as a result a well-ordered uniform ZnO-SS are obtained. The pictorial form of mechanism of formation of superstructures is shown in Figure 5a. Polysaccharides exhibit surface/interfacial activity; it has been attributed to the presence of protein impurities. Macromolecules combine polysaccharide and protein elements. The detailed study is needed to understand the formation of different ZnO-SS. The complexity and variety of polysaccharides can be explained by two ways, first monosaccharides can be linked together in different ways (1 to 2, 1 to 3, 1 to 4, 1 to 5 and 1 to 6, in an α and β configurations) and second due to the presence of branched side chains.[43,44] Many investigators have

DOI: 10.1021/sc500784p
ACS Sustainable Chem. Eng. 2015, 3, 1066−1080

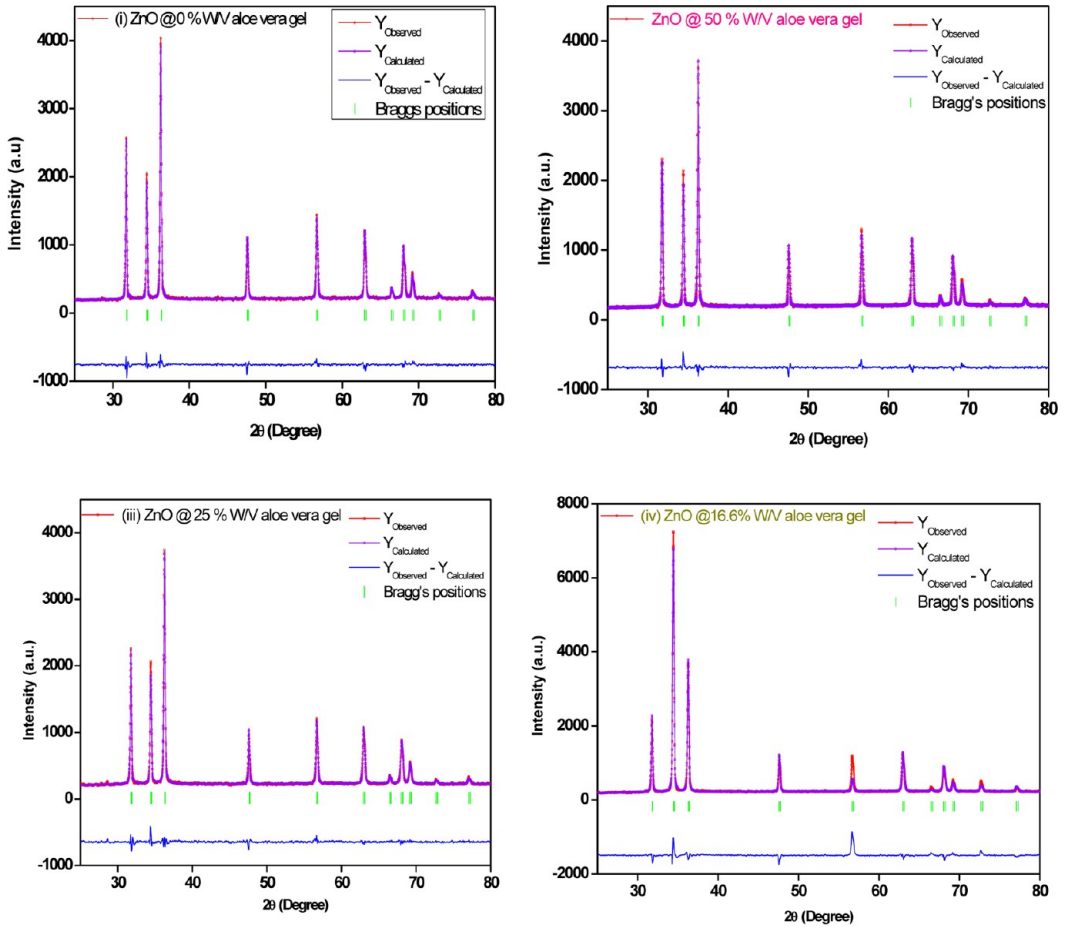

Figure 7. Rietveld refined profiles for ZnO with different aloe vera content.

Table 1. Crystal Data of ZnO for Different Aloe Vera Gel: JCPDS No. 89-7102

	ZnO without aloe vera	ZnO @ 50% W/V zinc nitrate with aloe vera gel	ZnO @ 25% W/V zinc nitrate with aloe vera gel	ZnO @ 16.6% W/V zinc nitrate with aloe vera gel
crystal structure	hexagonal	hexagonal	hexagonal	hexagonal
space group	*P*63*mc* (186)	*P*63*mc* (186)	*P*63*mc* (186)	*P*63*mc* (186)
Hall symbol	*P*6*c*$\bar{2}$*c*	*P*6*c*$\bar{2}$*c*	*P*6*c*$\bar{2}$*c*	*P*6*c*$\bar{2}$*c*
lattice parameters (Å)	*a* = 3.2462	*a* = 3.2458	*a* = 3.2467	*a* = 3.2451
	c = 5.2007	*c* = 5.1999	*c* = 5.2010	*c* = 5.1993
χ^2	0.926	0.974	1.094	1.171
*R*p	3.370	3.260	3.260	5.350
R_{Bragg}	4.320	3.410	3.570	11.30
R_{WP}	4.390	4.280	4.330	9.380
R_{exp}	4.740	4.390	3.958	8.010
volume of unit cell/formula unit (Å^3)	47.463	47.44	47.47	47.00
X-ray density (g/cm^3)	5.717	5.720	5.068	5.728
average crystallite size (nm) (from Scherrer formula)	11.49	11.37	11.34	11.40
aspect ratio in a and cdirections (D_a/D_c)	2.33	2.32	2.28	2.26

identified acemannan as the primary polysaccharide of the aloe vera gel,[45−47] while few reports mentioned as pectic substance as the primary polysaccharide.[48] Acemannan with the configuration *β*-(1,4)-glycosidic bond is important for its active reaction and pectic substance with amorphous carbohydrate present in aloe vera with chain of 1,4 linked *R*-D-galacturonic acid units interrupted by 1,2 linked L-rhamnopyranosyl residues in alternative positions acts as a biopolymer chain having a high anionic nature. During the process, pectin and acemannan serve as biotemplates to restrict the growth of ZnO structures, but also serve as assembling agents to get superstructures. Similarly cellulose, hemicelluloses, chitosan, xylan, etc. also contribute in stabilization of zinc ions to obtain various morphologies. The nature prefers the least utilization of energy in any of the self-assemblies. Hence in this method of preparation the supramolecular structures of ZnO are obtained by natures least energy utilization mechanisms.

DOI: 10.1021/sc500784p
ACS Sustainable Chem. Eng. 2015, 3, 1066−1080

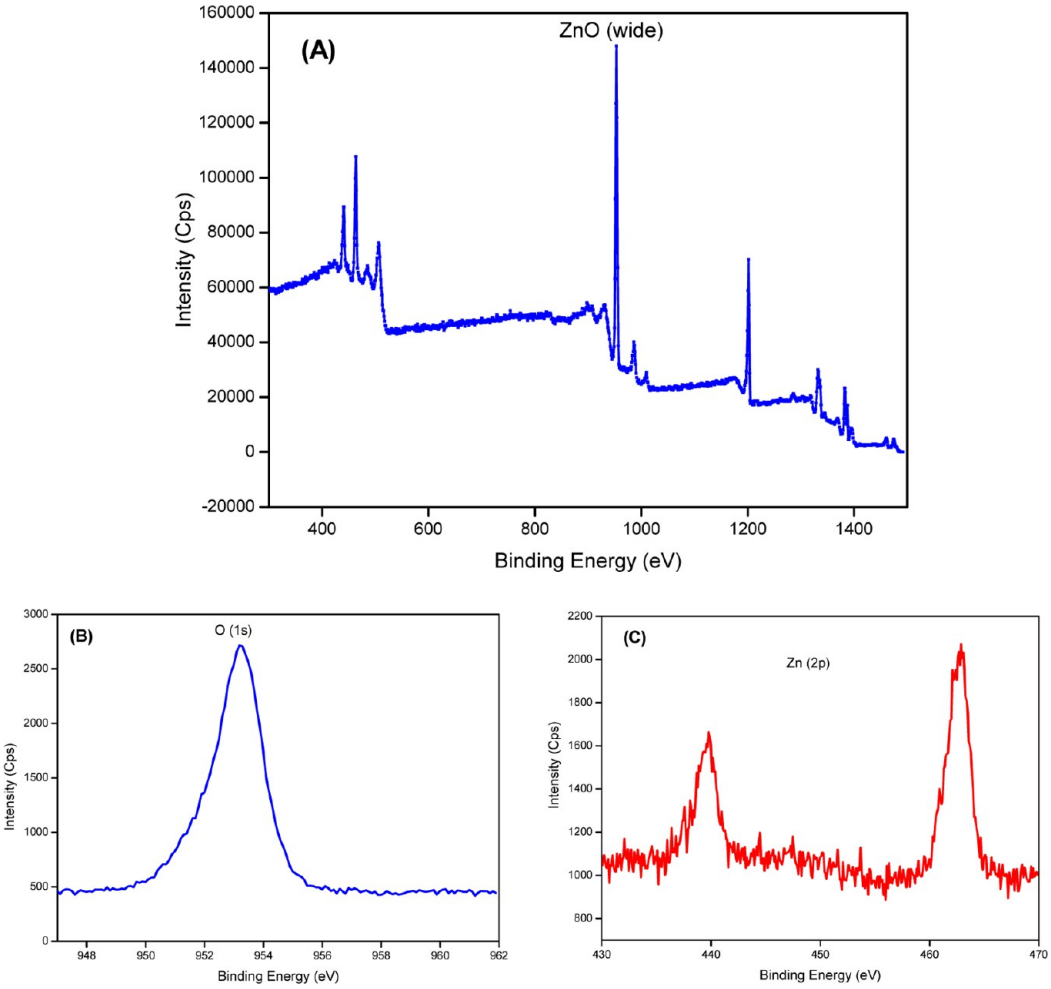

Figure 8. XPS spectra (A) wide range of binding energy spectrum, (B) O (1s) and (C) Zn (2p) elements of prepared ZnO using 16.6% W/V zinc nitrate with aloe vera gel.

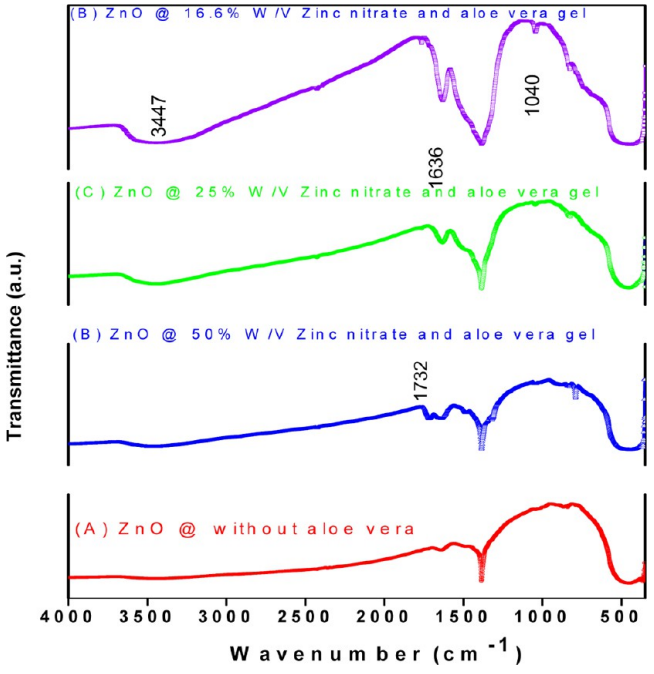

Figure 9. FTIR of synthesized ZnO-SS with various concentrations of aloe vera gel.

Different morphologies are obtained with different aloe vera content. The reason behind this is the polymeric network formed during the stirring process decomposed in an ordered manner when subjected to heat treatment during the combustion synthesis. The effective heat liberated during combustion process is in the layered manner and it may be interlocked with quantity of aloe vera content. At low temperatures, the rate of crystal growth is higher than the nucleation. Whereas, with increase in temperature, the nucleation rate gradually increases and overtakes the rate of crystalline growth. Hence, smaller sized and smoother surface structures would be produced at higher temperatures. In all the processes, the Zn^{2+} ions gets stabilized with various polysaccharide chains by interacting with O(-ve) ions. The overall mechanism involves some phenolic compounds, proteins that are bound to the surface of ZnO-SS during stirring process. The stability of ZnO-SS may be due to the free amino and carboxylic groups that have interacted with the zinc surface. The bonds of functional groups are derived from heterocyclic compounds of the protein chains. These functional groups act as capping ligands of the superstructures. Further, the proteins present in the medium prevent agglomeration and aids in the stabilization by forming a coat, covering the ZnO-SS.

The aloe vera gel mainly composed of sugar molecules such as glucose, galactose and acetylmanose, which are linked into chains of various lengths. The mechanism of incorporation of ZnO particles into the polysaccharide chains can be described by a

DOI: 10.1021/sc500784p
ACS Sustainable Chem. Eng. 2015, 3, 1066−1080

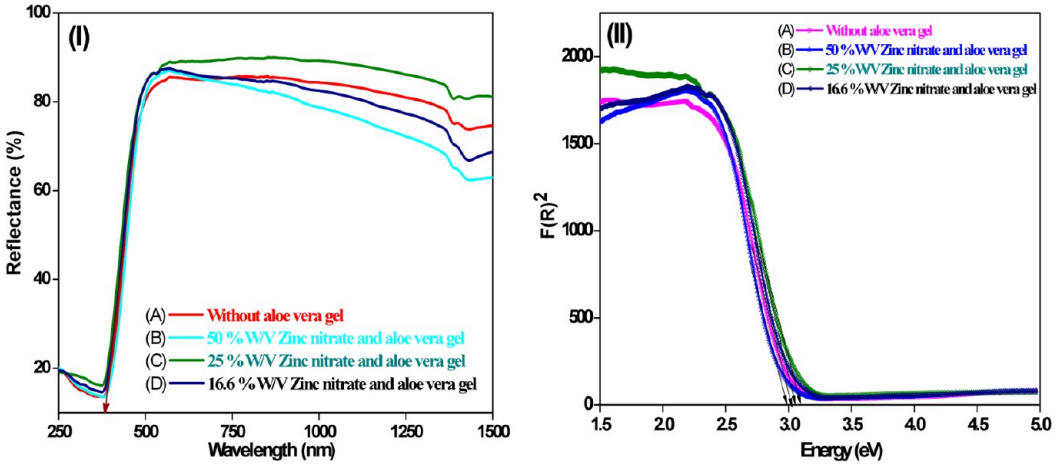

Figure 10. UV−visible spectra and energy band gap of ZnO-SS.

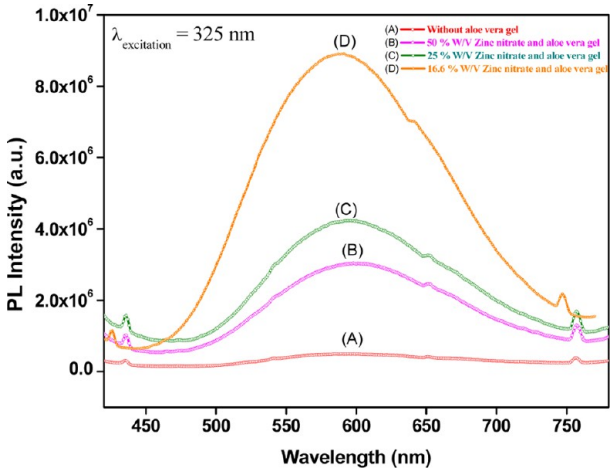

Figure 11. PL intensity of ZnO with different aloe vera concentration.

model called "egg box" (Figure 5b). This model consists of polysaccharide molecules that interact with trivalent/divalent cations, forming bridges between two carboxyl groups of acetyl groups from two different chains comes in close contact.[49,50] The divalent ions keep the molecules together and form superstructures along with supportive binding of two or more chains of polysaccharide. This mechanism forms the polymeric nature of bindings and their agglomeration further binds the ZnO+δ more strongly. This polymeric binding is responsible for the conjunction of all these families of compounds present in the gel and exhibit a synergistic effect to get the complex structures. Further, the interaction of proteins and polysaccharides as attractive or repulsive interaction, the synergistic effect fine-tunes.

It is well-known that ZnO belongs to the *P*63*mc* space group, and (0001) and (000-1) planes are rich in Zn (positive polar plane) and O (negative polar plane), respectively. These planes have different surface energies and thereby different growth rates.[51]The existence of some water-soluble organic compounds (phenols, terpenoids or proteins) present in aloe vera gel is adhered to the ZnO surface, thereby promoting the growth in a specific direction.[41,52,53] Figure 6 shows the powder X-ray diffraction (PXRD) patterns of ZnO-SS synthesized using various concentrations of aloe vera gel. All the diffraction peaks can be indexed to hexagonal wurtzite structure [JCPDS No. 89-7102] and space group *P*63*mc* (186) with slight variation in the lattice constants from the standard values (Table 1) confirms the formation of crystallite size. Though the aloe vera gel contains trace elements such as Fe, Cu, Zn, Mn, Al, Se and Cr, the PXRD pattern does not show any of the impurity peaks corresponding to the trace elements and their compounds. Generally, the (101) plane is dominant over the other planes. This result matches well with the previously report by Sangeetha et al., for the preparation of ZnO nano ZnO-SS using aloe vera gel as a surfactant via a precipitation method.[34] But in the present method of

Table 2. Antifungal Activity of ZnO-SS As Determined by the Agar Diffusion Method (diameter in mm) and Their Minimum Inhibitory Concentration (MIC) and Minimum Fungicidal Concentration (MFC) Analyzed by Microbroth Dilution Method

		zone of inhibition (mm)					
Sl no.	nanoparticle screened	1 mg·mL	0.5 mg·mL^{-1}	ketoconazole (positive control, 0.125 mg·mL^{-1})	ethanol (negative control)	MIC (mg·mL^{-1})	MFC (mg·mL^{-1})
1	ZnO @ 50% W/V zinc nitrate with aloe vera gel	13.625 ± 0.13	11.625 ± 0.13	24.00 ± 0.0	Nd[a]	0.008	0.016
2	ZnO @ 25% W/V zinc nitrate with aloe vera gel	22.5 ± 0.25	14.875 ± 0.13			0.016	0.125
3	ZnO @ 16.6% W/V zinc nitrate with aloe vera gel	23.25 ± 0.25	17.5 ± 0.25			0.066	0.132
4	ZnO without aloe vera gel	10.2 ± 0.33	Nd			0.500	1.000

[a]Nd: not detected.

DOI: 10.1021/sc500784p
ACS Sustainable Chem. Eng. 2015, 3, 1066−1080

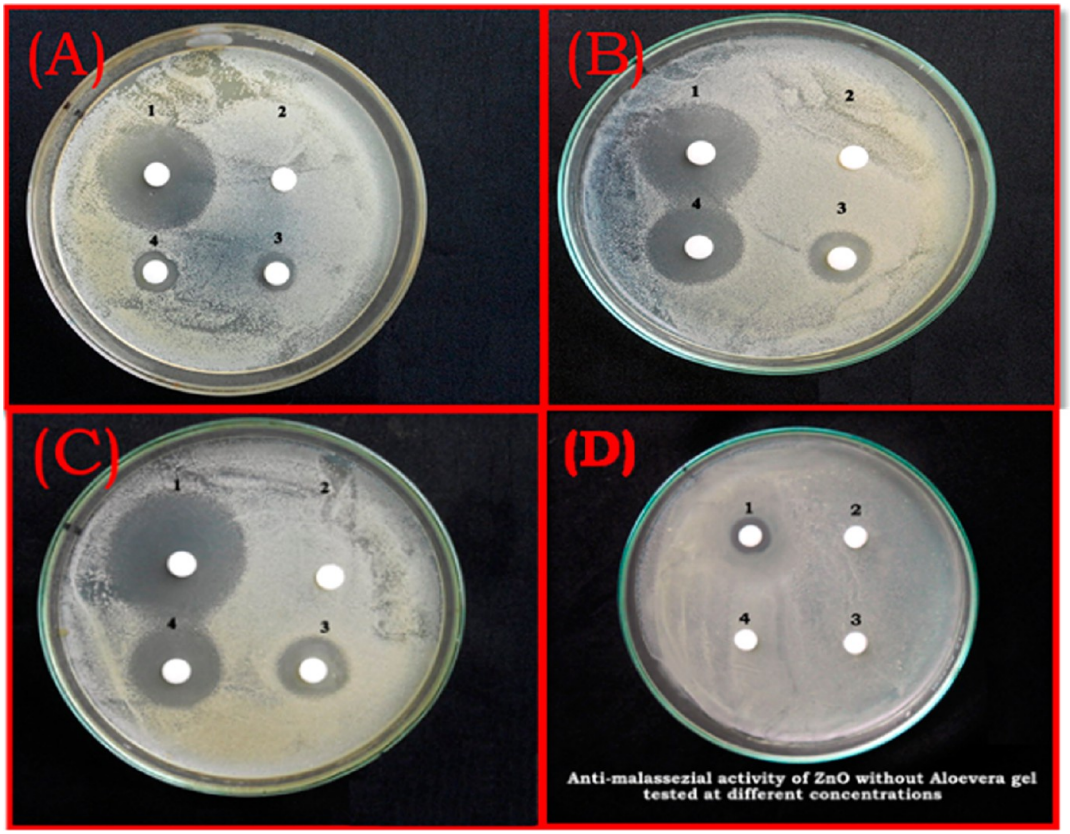

Figure 12. Antimalassezial activity of ZnO-SS on dermatologically prevalent yeast *M. furfur* (A) 50% W/V zinc nitrate and aloe vera gel, (B) 25% W/V zinc nitrate and aloe vera gel, (C) 16.6% W/V zinc nitrate and aloe vera gel [1, positive control; 2, negative control,3-0.5 mg/mL of ZnO and 4-1 mL/mg of ZnO-SS] and (D) ZnO without aloe vera gel [1-1 mg/mL; 2-0.5 mg/mL; 3-0.25 mg/mL of ZnO and 4, negative control].

preparation, with increase in the aloe vera content, the (002) plane becomes dominate over the other planes and shows the change in growth mechanism with concentration of the biotemplate. Further, it is observed that the preferred orientation of the (002) plane of the ZnO-SS obtained in the presence of aloe vera extract is slightly shifted to the lower angle side when compared to the without aloe vera used ZnO product (Figure 6B). In a more general way, the intensity depends on the number of atom layers correctly ordered perpendicular to the plane considered. It depends on the material and its preparation environment. In our case, due to the aloe vera gel as a surfactant, the reflections in the plane have almost constant intensities while the reflections due to the stacking in the *c*-axis may be very intense if a lot of layers are correctly ordered. As an intermediate situation, the intensity increases while ordering the stacking of the layers is observed with the increase in the aloe vera content. From the full widths at half-maximum (FWHMs) of major reflection peaks, the sizes of the coherently scattering domains in the "a" and "c" directions, Da and Dc, are calculated using Scherrer formula. Further, the aspect ratio (AR) = (D_a/D_c) is used to describe the anisotropy of the crystalline subunits of the agglomerations.[51] AR value decreased slightly with increase in aloe vera content and the average crystallite size is found to be ∼11 nm for all the compositions as listed in Table.1. The powder diffraction pattern is simulated with the help of the Rietveld's refinement software, the FULLPROF suite 2.05 program, by providing necessary structural information (Figure 7).[54] The background is successfully fitted with a Chebyshev function (χ^2) with a variable number of coefficients depending on its complexity and found good match. The detailed outputs of the refinement are tabulated in Table 1. The X-ray density is observed highest for ZnO prepared with 16.6% W/V zinc nitrate with aloe vera gel content. This may be attributed to the highest electron density for this composition of aloe vera.

The XPS of the ZnO prepared using 16.6% W/V zinc nitrate with aloe vera gel is as shown in Figure 8. Figure 8a shows the wide range of binding energy from 200 to 1500 eV and Figure 8b,c shows the narrow range of O (1S) and Zn (2p). The Zn(2p) XPS spectrum consists of Zn $^2p_{1/2}$ and $^2p_{3/2}$ doublet peak. The lower binding energy of 1022.2 eV corresponds to the Zn $^2p_{3/2}$ and the highest binding energy of 1045.6 eV corresponds to Zn $^2p_{1/2}$.[55] The O (1s) spectrum of the ZnO contains one peak due to the presence of oxide, hydroxides and adsorbed water. The intense peak is at 953.4 eV can be attributed to O^{2-} type of species associated with the oxide of Zn, which is in the form of ZnO. The intensity of the O (1s) peak shows that the amount of oxide associated with Zn is more than the hydroxide confirms that the formed compound is ZnO.

Figure 9 shows the FTIR analysis of ZnO-SS synthesized by a biotemplate method and ZnO prepared by a combustion method without using aloe vera content. The FTIR of pure ZnO does not show any traces of organic contents except the metal−oxygen bonding at ∼455 cm^{-1}, but the FTIR of ZnO prepared using aloe vera content revealed a strong band at 1396 cm^{-1}; however, the peak at 455 is related to Zn−O bond vibrational frequencies that support the presence of hexagonal phases. The bands at 3447 cm^{-1} show the presence of −OH stretching bonded to the Zn−OH. The bands at 1732 and 1636 cm^{-1} are due to traces of amide bonds of proteins/enzymes. Further, the bands observed at 1396 and 1040 cm^{-1} have been assigned to alcohols and phenolic

DOI: 10.1021/sc500784p
ACS Sustainable Chem. Eng. 2015, 3, 1066−1080

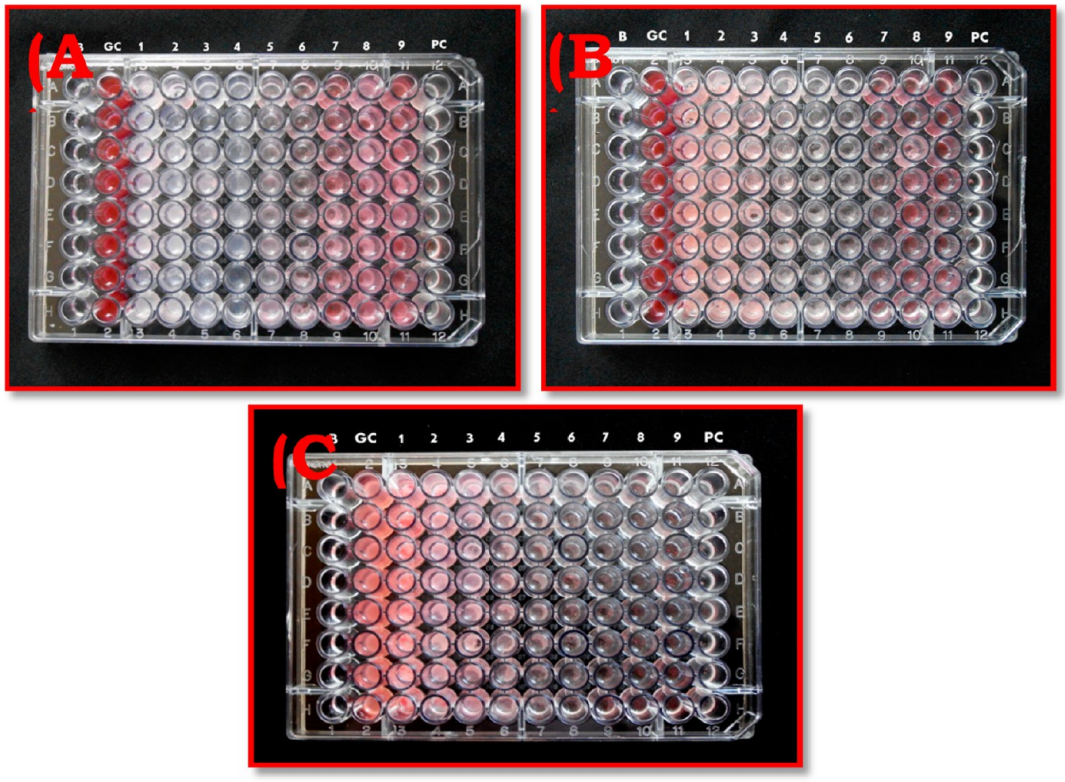

Figure 13. Determination of minimum inhibitory concentration (MIC) of ZnO-SS on *M. furfur* by 96-well plate method: (A) ZnO obtained using 50% W/V zinc nitrate with aloe vera gel; (B) ZnO obtained 25% W/V zinc nitrate with aloe vera gel and (C) ZnO obtained using 16.6% W/V zinc nitrate with aloe vera gel [B, blank; GC, growth control; PC, positive control; 1, 1; 2, 0.5; 3, 0.25; 4, 0.125; 5, 0.063; 6, 0.032; 7, 0.016; 8, 0.008; 9, 0.004 (mg/mL)].

groups, C−N stretching vibrations of aliphatic and aromatic amines, respectively.[34] The overall observation proves the existence of traces of some phenolic compounds, terpendoids or proteins that are bound to the surface of ZnO-SS that remained.

The optical properties of ZnO crystallites synthesized in the presence of aloe vera are observed in Figure 10A. In all the spectra, a strong decrease of reflectance can be noticed in the range of 360−385 nm corresponds to transitions in ZnO. Based on this reflectance data, the estimated band gap according to Kubela−Munk representation is shown in Figure 10B. The band gap values vary between 2.92 and 3.08 eV. The highest band gap of 3.08 eV is observed for ZnO prepared using 16.6% W/V zinc nitrate with aloe vera gel.[49]

Photoluminescence (PL) is an effective technique to assess both defects as well as optical property for possible applications in device fabrication. Figure 11 presents the photoluminescence spectra of the ZnO-SS synthesized using different concentrations of aloe vera gel with an excitation wavelength of 325 nm. PL spectra display two emission bands, the ultraviolet (UV) emission and the broad visible band. The UV peak attributed to the near-band-edge (NBE) emission, and the broad visible band is related to the deep-level defects formed by vacancies and interstitials of zinc or oxygen in ZnO.[56,57] Most of the ZnO nano/microstructures synthesized by wet chemical methods including hydrothermal, precipitation, sol−gel and solution combustion, so forth, exhibit broad blue, yellow or green emissions.[58] However, ZnO-SS synthesized using aloe vera plant gel exhibits unique and strong orange emission centered at 600 nm. It is widely accepted that the visible luminescence mainly originates from defect states such as Zn interstitial and oxygen vacancies. Thus, the peak at 600 nm is assigned to the electron transition from interstitial zinc to an interstitial oxygen (O_i) level.[59] It is important to mention that the ZnO-SS prepared by a precipitation method in the presence of aloe vera plant gel exhibits a green emission centered at 520 nm. The present study clearly suggests that the method of synthesis and type of nanostructure exhibit different optical properties. Further, it is observed that the emission intensity of ZnO-SS increases with increase in volume of aloe vera. As shown in Figure 11, the intensity ratio of the UV emission to the defect-related emission increases with respect to the rise in the aloe vera content except for 16.6% W/V zinc nitrate with aloe vera gel. This confirms the higher aspect ratio and better crystallinity for ZnO prepared using 16.6% W/V zinc nitrate with aloe vera gel. ZnO prepared using 16.6% W/V zinc nitrate with aloe vera gel concentration shows the highest PL intensity and for the same compound we observed the optimization in its SEM morphology, X-ray density, wide energy band gap and pure form of compound.

Qualitative and quantitative results determined using disc diffusion and broth microdilution methods are presented as average values in Table 2. The preliminary screening results of ZnO without aloe vera by disc diffusion showed the zone of inhibition of (10.2 ± 0.33) mm at 1 mg·mL^{-1}. *M. furfur* showed different degrees of sensitivity to different tested ZnO-SS and ZnO without aloe vera (Figure 12). Figure 12A for 50% W/V zinc nitrate with aloe vera gel concentration, Figure 12B for 25% W/V zinc nitrate with aloe vera gel concentration and Figure 12C shows the ZnO-SS obtained from 16.6% W/V zinc nitrate with aloe vera gel concentration. Among them, Figure 12C shows significantly a high inhibitory effect against the growth of *M. furfur* with MIC 0.008 mg/mL. The mean inhibition zone of all

DOI: 10.1021/sc500784p
ACS Sustainable Chem. Eng. 2015, 3, 1066−1080

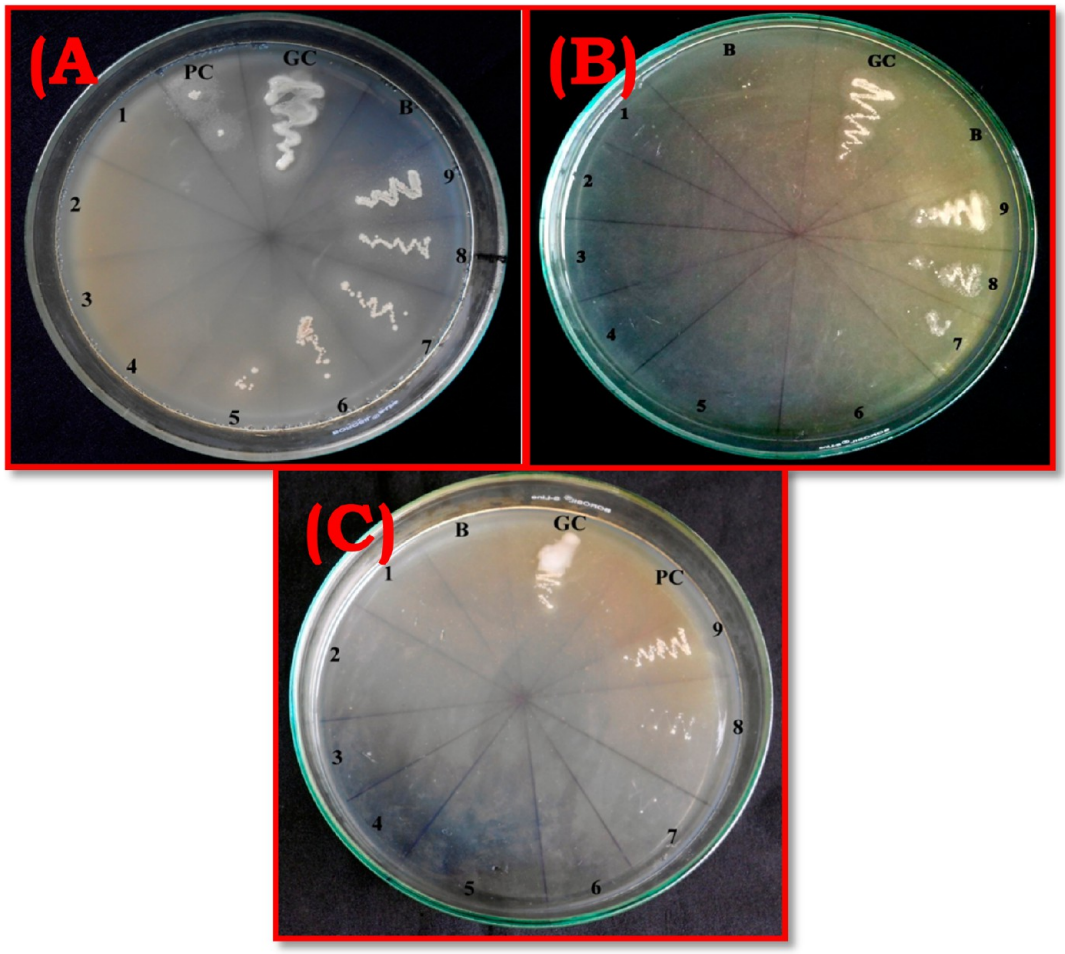

Figure 14. Determination of MIC and MYC of ZnO-SS on *M. furfur* by streak plate method. [B, blank; GC, growth control; PC, positive control; 1, 1; 2, 0.5; 3, 0.25; 4, 0.125; 5, 0.063; 6, 0.032; 7, 0.016; 8, 0.008; 9, 0.004 (mg/mL)].

the tested ZnO-SS ranged from 11 to 23 mm, indicating a remarkable antimalassezial effect when compared with that of ketoconazole with 24 mm tested at 0.125 mg/mL. To determine the MIC, concentrations of the ZnO-SS varying between 1 and 0.04 mg·mL^{-1} were tested. On 96-well microdilution followed by conformational streaking, it was found that ZnO without aloe vera exhibited a higher MIC of 0.500 mg/mL, which was relatively high compared with ZnO-SS, which showed the MIC range of 0.008 to 0.063 mg/mL when tested at different concentrations of zinc nitrate with aloe vera gel. The pronounced antifungal activity of ZnO-SS can be due to its relatively small size and high surface to volume ratios compared with Zinc oxide without aloe vera. The present study clearly signifies the potentiality of ZnO-SS as antifungal agents over ZnO without aloe vera gel. Table 2 and Figure 13 show the different zones of inhibition with MIC and MFC of the extracts against the organism. Figure 14 shows the determination of MIC and MYC of ZnO-SS on *M. furfur* by the streak plate method.

To know the morphological changes that could be attributed to antimalassezial activity, inclusion−exclusion using fluorochromes viz Acridine orange (AO)/Ethidium bromide (EB) dyes is used. Live and Dead cells were identified by nuclear condensation of chromatin stained by AO (green color) or EB (orange color), respectively; thereby indicating cell membrane damage. Dead cells were identified by uniform labeling of the cells with EB. Live cells were dispersed and alive with normal nuclei staining that present yellowish to green chromatin (Figure 15D) with organized structures. The yeast cells treated with ZnO-SS have similar normal nuclei staining as live cells except the chromatin is orange instead of green, showcasing the cell aggregation (Figure 15A,B,C), suggesting that ZnO-SS has immense potential as an antifungal agent.

CONCLUSIONS

Aloe vera gel assisted solution combustion method is a fast, simple, convenient, economical and environmentally benign method compared to the previously reported conventional solution combustion syntheses. The ZnO without aloe vera is very reluctant to the antifungal activity, whereas ZnO-SS with different aloe vera concentrations showed better antifungal activity for a least concentration of about 0.5 mg/mL. The synthesized ZnO-SS show highest band gap and purest form when synthesized with 16.6% W/V zinc nitrate with aloe vera gel concentration. The synthesized ZnO-SS exhibits unique orange emission at 600 nm. The yeast cells treated with ZnO-SS have similar normal nuclei staining as live cells, except the chromatin is orange instead of green, showcasing the cell aggregation and suggesting that ZnO-SS has immense potential as an antifungal agent. Hence, the explored method of preparation shows that highly efficient ZnO-SS derived from aloe vera plant gel is expected to have extensive applications in the medical, biomedical and cosmetic industries.

DOI: 10.1021/sc500784p
ACS Sustainable Chem. Eng. 2015, 3, 1066−1080

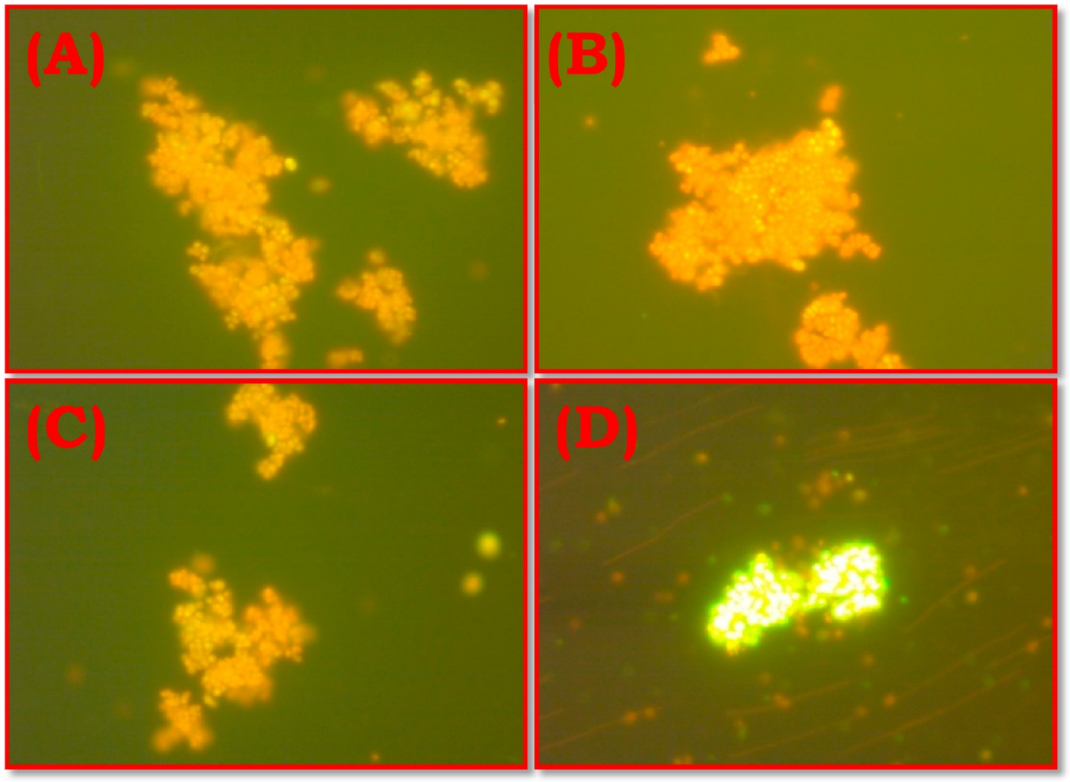

Figure 15. Fluorescence imaging of *M. furfur* treated with (A) ZnO @ 50% W/V zinc nitrate with aloe vera gel, (B) ZnO @ 25% W/V zinc nitrate with aloe vera gel, (C) ZnO @ 16.6% W/V zinc nitrate with aloe vera gel and (D) cells without treatment.

AUTHOR INFORMATION

Corresponding Author

*H. Nagabhushana. E-mail: bhushanvlc@gmail.com. Tel.: +91-9663177440.

Notes

The authors declare no competing financial interest.

ACKNOWLEDGMENTS

Dr. H. Nagabhushana thanks DST Nano Mission (Project No. SR/NM/NS-48/2010) New Delhi for the sanction of this project.

REFERENCES

(1) Donnarumma, G.; Perfetto, B.; Paoletti, I.; Oliviero, G.; Clavaud, C.; Del Bufalo, A.; Breton, L. Analysis of the response of human keratinocytes to Malassezia globosa and restricta strains. *Arch. Dermatol. Res.* **2014**, *306*, 763−768.

(2) Gupta, A. K.; Lyons, D. C. Pityriasis versicolor: An update on pharmacological treatment options. *Expert Opin. Pharmacother.* **2014**, *15*, 1707−1713.

(3) Rubenstein, R. M.; Malerich, S. A. Malassezia (Pityrosporum) Folliculitis. *J. Clin. Aestheth. Dermatol.* **2014**, *7*, 37−41.

(4) Buechner, S. A. Multicenter, double-blind, parallel group study investigating the non-inferiority of efficacy and safety of a 2% miconazole nitrate shampoo in comparison with a 2% ketoconazole shampoo in the treatment of seborrhoeic dermatitis of the scalp. *J. Dermatol. Treat.* **2014**, *25*, 226 −231.

(5) Brzezinski, P. T.; Pinteala, A. E.; Chiriac, L.; Foia, A. Chiriac, Aplasia cutis congenita of the scalp - What are the steps to be followed? Case report and review of the literature. *An. Bras. Dermatol.* **2015**, *90*, 100−103.

(6) Rudramurthy, S. M.; Honnavar, P.; Chakrabarti, A.; Dogra, S.; Singh, P.; Handa, S. Association of Malassezia species with psoriatic lesions. *Mycoses* **2014**, *57*, 483−488.

(7) Hawkins, D. M.; Smidt, A. C. Superficial fungal infections in children. *Pediatr. Clin. North Am.* **2014**, *61*, 443−455.

(8) Arsenijevic, V. S. A.; Milobratovi, D.; Bara, A. M.; Veki, B.; Marinkovi, J.; Kosti, V. S. A laboratory-based study on patients with Parkinson's disease and seborrheic dermatitis: The presence and density of Malassezia yeasts, their different species and enzymes production. *BMC Dermatol.* **2014**, *5*, 1−9.

(9) Bulmer, A. C.; Bulmer, G. S. The antifungal action of dandruff shampoos. *Mycopathologia* **1999**, *147*, 63−65.

(10) Diaz-Visurraga, J.; Gutierrez, C.; Von Plessing, C.; Garcia, A. Metal nanostructures as antibacterial agents. *Sci. Technol. Microb. Pathog., Proc. Int. Conf. Antimicrob. Res.* **2011**, *3*, 210−218.

(11) Nel, A. E.; Madler, L.; Velegol, D.; Xia, T.; Hoek, E. M.; Somasundaran, P.; Klaessig, F.; Castranova, V.; Thompson, M. Understanding biophysicochemical interactions at the nano−bio interface. *Nat. Mater.* **2009**, *8*, 543−557.

(12) Linkov, I.; Satterstrom, K.; Corey, L. Nanotoxicology and nanomedicine: Making hard decisions. *Nanomedicine* **2008**, *4*, 167−171.

(13) Mccune, M.; Zhang, W.; Deng, Y. High efficiency dye-sensitized solar cells based on three-dimensional multi-layered ZnO nanowire arrays with "caterpillar-like" structure. *Nano Lett.* **2012**, *11*, 3656−3662.

(14) Wang, J. X.; Sun, X. Y.; Yang, Y.; Huang, H.; Lee, Y. C.; Tan, O. K.; Vayssieres, L. Hydrothermally grown oriented ZnO nanorod arrays for gas sensing applications. *Nanotechnology* **2006**, *17*, 4995−4998.

(15) Liu, J.; Wu, W.; Bai, S.; Qin, Y. Synthesis of high crystallinity ZnO nanowire array on polymer substrate and flexible fiber-based sensor. *ACS Appl. Mater. Interfaces* **2011**, *3*, 4197−4200.

(16) Su, Y. K.; Peng, S. M.; Ji, W.; Wu, L. C. Z.; Cheng, W. B.; Liu, C. H. Ultraviolet ZnO nanorod photosensors. *Langmuir* **2010**, *26*, 603−606.

(17) Ahmad, M.; Zhu, J. ZnO based advanced functional nanostructures: Synthesis, properties and applications. *J. Mater. Chem.* **2010**, *21*, 599−614.

(18) Baruah, S.; Jaisai, M. Photocatalytic paper using zinc oxide nanorods. *Sci. Technol. Adv. Mater.* **2010**, *11*, 055002.

(19) Sadhasivum, S.; Shanmugam, P.; Yun, K. Biosynthesis of silver nanoparticles by Streptomyces hygroscopicus and antimicrobial activity

DOI: 10.1021/sc500784p
ACS Sustainable Chem. Eng. 2015, 3, 1066−1080

against medically important pathogenic microorganisms. *Colloids Surf., B* **2010**, *81*, 358−362.
(20) Tayel, A. A.; EL-TRAS, W. F.; Moussa, S.; EL-BAZ, A. F.; Mahrous, H.; Salem, M. F.; Brimer, L. Antibacterial action of zinc oxide nanoparticles against foodborne pathogens. *J. Food Safety* **2011**, *31*, 211−218.
(21) Lakshmeesha, T. R.; Sateesh, M. K.; Daruka Prasad, B.; Sharma, S. C.; Kavyashree, D.; Chandrasekhar, M. H.; Nagabhushana, H. Reactivity of crystalline ZnO superstructures against fungi and bacterial pathogens: Synthesized using Nerium oleander leaf extract. *Cryst. Growth Des.* **2014**, *14*, 4068−4079.
(22) Yousef, J. M.; Danial, E. N. *In vitro* antibacterial activity and minimum inhibitory concentration of zinc oxide and nano-particle zinc oxide against pathogenic strains. *J. Health Sci.* **2012**, *2*, 38−42.
(23) Panatarani, C.; Lenggoro, I. W.; Okuyama, K. Synthesis of single crystalline ZnO nanoparticles by salt-assisted spray pyrolysis. *J. Nanoparticle Res.* **2003**, *5*, 47−53.
(24) Paez, J. E. R.; Caballero, A. C.; Villegas, M. Controlled precipitation methods: Formation mechanism of ZnO nanoparticles. *J. Eur. Ceram. Soc.* **2011**, *21*, 925−930.
(25) Liu, B.; Zeng, H. C. Hydrothermal synthesis of ZnO nanorods in the diameter regime of 50 nm. *J. Am. Chem. Soc.* **2003**, *125*, 4430−4431.
(26) Wu, J. J.; Liu, S. C. Catalyst-free growth and characterization of ZnO nanorods. *Adv. Mater.* **2002**, *14*, 215−218.
(27) Tissot, I.; Reymond, J. P.; Lefebvre, F.; Bourgeat-lami, E. SiOH-functionalized polystyrene latexes. A step toward the synthesis of hollow silica nanoparticles. *Chem. Mater.* **2002**, *14*, 1325−1331.
(28) Zhang, Y.; Jia, H. B.; Wang, R. M.; Chen, C. P.; Luo, X. H.; Yu, D. P.; Lee, C. Low-temperature growth and Raman scattering study of vertically aligned ZnO nanowires on Si substrate. *J. Appl. Phys. Lett.* **2003**, *83*, 4631−4633.
(29) Hari Krishna, R.; Nagabhushana, B. M.; Nagabhushana, H.; Suriya Murthy, N.; Sharma, S. C.; Shivakumara, C.; Chakradhar, R. P. S. Effect of calcination temperature on structural, photoluminescence, and thermoluminescence properties of Y_2O_3:Eu^{3+} nanophosphor. *J. Phys. Chem. C* **2013**, *117*, 1915−1924.
(30) Nagappa, B.; Chandrappa, G. T. Mesoporous nanocrystalline magnesium oxide for environmental remediation. *Micropor. Mesopor. Mater.* **2007**, *106*, 212−218.
(31) Chandran, S. P.; Chaudhary, M.; Pasricha, R.; Ahmad, A.; Sastry, M. Synthesis of gold nanotriangles and silver nanoparticles using aloe vera plant extract. *Biotechnol. Prog.* **2006**, *22*, 577−583.
(32) Sangeetha, G.; Rajeshwari, S.; Venckatesh, R. Green synthesis of zinc oxide nanoparticles by aloe barbadensis miller leaf extract: Structure and optical properties. *Mater. Res. Bull.* **2011**, *46*, 2560−2566.
(33) Phumying, S.; Labuayai, S.; Thomas, C.; Amornkitbamrung, V.; Swatsitang, E.; Maensiri, S. Aloe vera plant-extracted solution hydrothermal synthesis and magnetic properties of magnetite (Fe_3O_4) nanoparticles. *Appl. Phys. A: Mater. Sci. Process.* **2013**, *111*, 1187−1193.
(34) Maensiri, S.; Laokul, P.; Klinkaewnarong, J.; Phokha, S.; Promarak, V.; Seraphin, S. J. Indium oxide (In_2O_3) nanoparticles using aloe vera plant extract: Synthesis and optical properties. *Optoelectron. Adv. Mater.* **2008**, *10*, 161−165.
(35) Patel, V. K.; Bhattacharya, S. High-performance nanothermite composites based on aloe-vera directed CuO nanorods. *ACS Appl. Mater. Interfaces* **2013**, *5*, 13364−13374.
(36) Leeming, J. P.; Notman, F. H. Improved methods for isolation and enumeration of Malassezia furfur from human skin. *J. Clin. Microbiol* **1987**, *25*, 2017−2019.
(37) Samie, A.; Tambani, T.; Harshfield, E.; Green, E.; Ramalivhana, J. N.; Bessong, P. O. Antifungal activities of selected Venda medicinal plants against Candida albicans, Candida krusei andCryptococcus neoformans isolated from South African AIDS patients. *Afr. J. Biotechnol.* **2010**, *9*, 2965−2976.
(38) Ruppova, K.; Wsolova, L.; Sedlak, J.; Horvathova, M.; Urbancikova, M. Detection of apoptotic changes in HeLa cells after treatment with paracetamol. *Gen. Physiol. Biophys.* **1999**, *18*, 140−146.
(39) Ribble, D.; Goldstein, N. B.; Norris, D. A.; Shellman, Y. G. A simple technique for quantifying apoptosis in 96-well plates. *BMC Biotechnol.* **2005**, *5*, 12. DOI: 10.1186/1472-6750-5-12.
(40) Sui, M.; Zhang, L.; Sheng, L.; Huang, S.; She, L. Synthesis of ZnO coated multi-walled carbon nanotubes and their antibacterial activities. *Sci. Total Environ.* **2013**, *452*, 148−154.
(41) Huang, J.; Li, Q.; Sun, D.; Lu, Y.; Su, Y.; Yang, X.; Wang, H.; Wang, Y.; Shao, W.; He, N.; Hong, J.; Chen, C. Biosynthesis of silver and gold nanoparticles by novel sundried Cinnamomum camphora leaf. *Nanotechnology* **2007**, *18*, 105104.
(42) Maliyekkal, S. M.; Anshup, K. R.; Antony; Pradeep, T. High yield combustion synthesis of nanomagnesia and its application for fluoride removal. *Sci. Total Environ.* **2010**, *408*, 2273−2282.
(43) Neemann, F.; Rosenberger, S.; Jefferson, B.; McAdam, E. J. Non-covalent protein-polysaccharide interactions and their influence on membrane fouling. *J. Membr. Sci.* **2013**, *446*, 310−317.
(44) Rodriguez patino, J. M.; Pilosof, A. M. R. Protein-polysaccharide interactions at fluid interfaces. *Food Hydorcolloids* **2011**, *25*, 1925−1937.
(45) Ni, Y.; Turner, D.; Yates, K. M.; Tizard, I. Isolation and characterization of structural components of aloe vera L. leaf pulp. *Int. Immunopharmacol.* **2004**, *4*, 1745−1755.
(46) Rezaie, A.; Ebadi, A.; Nazeri, M.; Rezaie, S.; Elmi, F. Effect of aloe vera on healing of the experimental skin wounds on rats and its comparison with zinc oxide: A geometry and histopathologic study. *J. Anim. Vet. Adv.* **2012**, *11*, 2445−2452.
(47) Hamman, J. H. Composition and applications of aloe vera leaf gel. *Molecules* **2008**, *13*, 1599−1616.
(48) Wang, A.; Liao, Q.; Feng, J.; Zhang, P.; Li, A.; Wang, J. Apple pectin-mediated green synthesis of hollow double-caged peanut-like ZnO hierarchical superstructures and photocatalytic applications. *Cryst. Eng. Comm.* **2012**, *14*, 256−263.
(49) Preda, N.; Enculescu, M.; Enculescu, I. Polysaccharide-assisted crystallization of ZnO micro/nanostructures. *Mater. Lett.* **2014**, *115*, 256−260.
(50) Vasile, B. S.; Oprea, O.; Voicu, G.; ficai, A.; Andronescu, E.; Teodorescu, A.; Holban, A. Synthesis and characterization of a novel controlled release zinc oxide/gentamicin-chitosan composite with potential applications in wounds care. *Int. J. Pharm.* **2014**, *463*, 161−169.
(51) Waltz, F.; Wibmann, G.; Lippke, J.; Schneider, A. M.; Schwarz, H.; feldhoff, A.; Eiden, S.; Behrens, P. Evolution of the morphologies of zinc oxide mesocrystals under the influence of natural polysaccharides. *Cryst. Growth Des.* **2012**, *12*, 3066−3075.
(52) Sastry, M.; Ahmad, A.; Khan, M. I.; Kumar, R. Biosynthesis of metal nanoparticles using fungi and actinomycete. *Curr. Sci.* **2003**, *85*, 162−170.
(53) Sanghi, R.; Verma, P. Biomimetic synthesis and characterisation of protein capped silver nanoparticles. *Bioresour. Technol.* **2009**, *100*, 501−504.
(54) Daruka Prasad, B.; Nagabhushana, H.; Thyagarajan, K.; Nagabhushana, B. M.; Jnaneshwara, D. M.; Sharma, S. C.; Shivakumara, C.; Gopal, N. O.; Ke, S.; Chakradhar, R. P. S. Magnetic and dielectric interactions in nano zinc ferrite powder: Prepared by self-sustainable propellant chemistry technique. *J. Mag. Mag. Mater.* **2014**, *358*−*359*, 132−141.
(55) Moulder, J.F.; Stickle, W.F.; Sobol, P.E.; Bomben, K.D. In *Hand Book of X-ray Photoelectron Spectroscopy*; Chastain, J., Ed.; PerkinElmer Corporation: Eden Prairie, MN, 1992.
(56) Qiu, J.; Li, X.; He, W.; Park, S.-J; Kim, H.-K; Hwang, Y.-H; Lee, J.-H; Kim, Y.-D. The growth mechanism and optical properties of ultralong ZnO nanorod arrays with a high aspect ratio by a preheating hydrothermal method. *Nanotechnology* **2009**, *20*, 155603.
(57) Sreekantan, S.; Gee, L. R.; Lockman, Z. Room temperature anodic deposition and shape control of one-dimensional nanostructured zinc oxide. *J. Alloys Compd.* **2009**, *476*, 513−518.
(58) Jiang, C.; Zhang, W.; Zou, G.; Yu, W.; Qian, Y. Precursor-induced hydrothermal synthesis of flowerlike cupped-end microrod bundles of ZnO. *J. Phys. Chem. B* **2005**, *109*, 1361−1363.

DOI: 10.1021/sc500784p
ACS Sustainable Chem. Eng. 2015, 3, 1066−1080

(59) Ahn, C. H.; Kim, Y. Y.; Kim, D. C.; Mohanta, S. K.; Cho, H. K. A comparative analysis of deep level emission in ZnO layers deposited by various methods. *J. Appl. Phys.* **2009**, *105*, 013502−013505.

DOI: 10.1021/sc500784p
ACS Sustainable Chem. Eng. 2015, 3, 1066−1080